



Published in final edited form as:

Anal Chem. 2009 December 15; 81(24): 9985–9992. doi:10.1021/ac901833s.

Mixed Monolayers of Ferrocenylalkanethiol and Encapsulated Horseradish Peroxidase for Sensitive and Durable Electrochemical Detection of Hydrogen Peroxide

Yong Peng^{↑, #}, Dianlu Jiang[↑], Lei Su[↑], Lin Zhang^{↑, #}, Ming Yan[‡], Juanjuan Du[‡], Yufeng Lu[‡], You-Nian Liu^{*, #}, and Feimeng Zhou^{*, ↑}

[↑]Department of Chemistry and Biochemistry, California State University, Los Angeles, Los Angeles, California 90032

[#]College of Chemistry and Chemical Engineering, Central South University, Changsha, Hunan, P. R. China 410083

[‡]Department of Chemical and Biomolecular Engineering, University of California, Los Angeles, Los Angeles, CA 90095

Abstract

This paper describes the construction of a mixed monolayer of ferrocenylalkanethiol and encapsulated horseradish peroxidase (HRP) at a gold electrode for amperometric detection of H₂O₂ at trace levels. By tuning the alkanethiol chain lengths that tether the HRP enzyme and the ferrocenylalkanethiol (FcC₁₁SH) mediator, facile electron transfer between FcC₁₁SH and HRP can be achieved. Unlike most HRP-based electrochemical sensors, which rely on HRP-facilitated H₂O₂ reduction (to H₂O), the electrocatalytic current is resulted from an HRP-catalyzed oxidation reaction of H₂O₂ (to O₂). Upon optimizing other experimental conditions (surface coverage ratio, pH, and flow rate), the electrocatalytic reaction proceeding at the electrode was used to attain a low amperometric detection level (0.64 nM) and a dynamic range spanning over three orders of magnitude. Not only does the thin hydrophilic porous HRP capsule allow facile electron transfer, it also enables H₂O₂ to permeate. More significantly, the enzymatic activity of the encapsulated HRP is retained for a considerably longer period (> three weeks) than naked HRP molecules attached to an electrode or those wired to a redox polymer thin film. By comparing to electrodes modified with denatured HRP that are subsequently encapsulated or embedded in a poly-L-lysine matrix, it is concluded that the encapsulation has significantly preserved the native structure of HRP and therefore its enzymatic activity. The electrode covered with FcC₁₁SH and encapsulated HRP is shown to be capable of rapidly and reproducibly detecting H₂O₂ present in complex sample media.

Introduction

One of the forefronts of analytical chemistry is the development of heterogeneous enzyme biosensors wherein enzymes are immobilized onto solid surfaces and used to generate signals corresponding to specific analytes in solution.^{1–4} Since efficient catalytic activity at surface largely governs the ultimate performance of an enzyme biosensor, retention of the enzymatic activity and prevention of enzyme leaching are two important criteria for constructing successful sensors.^{5, 6} In general, to avoid serious enzyme leaching from the surface, covalent linkage of enzyme molecules onto surface is more advantageous than physical adsorption. As for retaining the enzymatic activity, numerous strategies have been explored. These strategies

*Corresponding authors. liuyoun@mail.csu.edu.cn (Y.-N. L.) and fzhou@calstatela.edu (F. Z.).

include, but are not limited to, entrapment of enzyme molecules in sol-gel,^{7, 8} hydrogel,⁹ conducting or redox polymer matrices^{10, 11} and nanoporous materials,^{12, 13} attachment of enzymes onto highly hydrophilic surfaces (e.g., polylysine,¹⁴ polyethylene glycol,^{15, 16} chitosan,^{17, 18} and dextran,^{19, 20}), and separation of enzyme layers from sample solutions using polymeric membranes^{21, 22}, and ion-exchange polyion membranes.^{23, 24}

Several recent papers have described the synthesis of “single-enzyme nanoparticles (SENs)” in bulk and applications of them to study enzymatic reactions in homogeneous solutions. The common procedure resorts to coupling monomers onto certain residues of an enzyme molecule, followed by initiation of polymerization of monomers (e.g., acrylamide) and cross-linking of the resultant polymer into a network. As a result, individual enzyme molecules are encapsulated into a polymeric and hydrophilic exterior. Kim and Grate were the first to encapsulate trypsin and chymotrypsin with a porous vinyl polymer/siloxane network and demonstrated that small molecules can readily move across the shell to reach the enzyme molecules.²⁵ A particularly attractive feature is that the encapsulated enzymes sustain their activities over an extended period of time. Using HRP as a model system, Liu and coworkers enclosed single horseradish peroxidase (HRP) molecules in a nanogel shell and showed that the shell thickness can be augmented via further polymerization of acrylamide monomers added in solution.²⁶ Lin, Wang, and coworkers immobilized HRP nanoparticles comprising of over 1000 cross-linked HRP molecules onto an electrode and achieved a mediator- and promoter-free electrochemical detection of H₂O₂ at micromolar concentrations.²⁷ Interestingly, encapsulated single HRP molecules have not been immobilized at a solid substrate and utilized as part of a heterogeneous biosensor for durable detection at low H₂O₂ concentrations.

We wish to report the modification of gold electrodes with a mixed monolayer of ferrocenylalkanethiol/encapsulated HRP for sensitive amperometric H₂O₂ detection. Instead of forming the HRP capsules in a homogeneous solution, enclosure of the HRP molecules with a porous, hydrophilic shell is carried out “in-situ” at the electrode interface. The ferrocenylalkanethiol serves as a mediator for generating a large electrocatalytic current. We found that the ferrocene group located at the end of the alkyl chain, with an oxidation potential higher than ferrocene or its derivative in solution, participates in an HRP-catalyzed H₂O₂ oxidation reaction to O₂. This is in contrast to many previously studied mediators in solution, which tend to partake in HRP-catalyzed H₂O₂ reduction reaction to produce H₂O.^{28–33} In addition to preserving the HRP enzymatic activity and enabling the analyte permeability across the capsule, we also show that, through optimizing lengths of the molecules tethering the HRP and mediator molecules and the enzyme/mediator ratio in the mixed monolayer, facile electron transfer between the HRP and ferrocenylalkanethiol molecules can be achieved. As a result, a remarkable sensitivity for electrochemical H₂O₂ detection is obtained and the robustness of the electrode is demonstrated to be suitable for H₂O₂ measurement in complex sample media.

Experimental Section

Materials

11-Ferrocenyl-1-undecanethiol (Fc-C₁₁SH) was purchased from Dojindo Laboratories (Kumamoto, Japan). *N*-(3-dimethylaminopropyl)-*N*'-ethylcarbodiimide hydrochloride (EDC), *N*-hydroxysuccinimide (NHS), 3-mercaptopropionic acid (MPA), horseradish peroxidase VI (HRP), poly-L-lysine, and hydrogen peroxide were acquired from Sigma-Aldrich (St. Louis, MO). *N*-acryloxysuccinimide, 4-dimethylaminoantipyrine (DMAP), ammonium persulfate, *N,N,N',N'*-tetramethylethylenediamine, acrylamide, *N,N'*-methylene bisacrylamide, 4-dimethylaminoantipyrine, and boric acid were obtained from Thermo-Fisher Scientific (Pittsburgh, PA). 2,2'-Bipyridineruthenous dichloride (Ru(bpy)₃Cl₂) was obtained from Simth G. Frederick Chemical Company (Powell, OH). Aqueous solutions were prepared using Millipore water (18 MΩ•cm, Simplicity Model, Billerica, MA). The wired HRP/polymer

solution for preparing the electrode was purchased from Bioanalytical System Inc. (BAS, West Lafayette, IN).

Instrumentation

Electrochemical experiments in quiescent solutions or flowing solution streams were carried out using a CHI-832 electrochemical workstation (CH Instruments, Austin, TX). Polycrystalline, 3 mm diameter gold disk working electrodes (BAS), a Ag/AgCl reference electrode (BAS), and a platinum coil auxiliary electrode were used in preliminary studies on the electrode reaction mechanism. A 3 mm gold disk embedded in a flat PEEK block (BAS) served as the working electrode for the amperometric detection of H₂O₂. The design of the homemade thin-layer flow cell is analogous to that of the commercially available flow cell (CH Instruments), except that a stainless steel tubing (1/16" OD, 0.02" ID and 4" long) was connected to the outlet of the cell as the auxiliary electrode.

Procedures

Electrode Modification—Gold disk electrodes were cleaned electrochemically in 0.1 M sulfuric acid by cycling potential between 0.0 and 2.0 V vs. Ag/AgCl for 10 min, rinsing with water and drying under nitrogen. This was followed by immersing the electrodes in 60 μL of dimethyl sulfoxide (DMSO) containing 0.83 mM FcC₁₁SH and 4.2 mM MPA for 1 h. Then, the electrodes were submerged in a 2.5 mM MPA solution for 1 h to obtain an optimal FcC₁₁SH coverage. To attach HRP, the electrodes were first kept in 60 μL of phosphate buffered saline (PBS, pH 5.5) containing 75 mM EDC and 15 mM NHS for 0.5 h. Subsequently they were soaked in 2 mg/mL HRP solution (pH 5.5) overnight. To encapsulate HRP, the electrodes covered with FcC₁₁SH/HRP were first submerged in 3.8 mL of borate buffer (100 mM, pH = 9.3) that also contained 0.5 mg 4-dimethylaminoantipyrine.³⁴ Next, 0.2 mL DMSO comprising 4.0 mg *N*-acryloxysuccinimide was gradually added and the reaction was allowed to proceed for 2 h at room temperature. After acryloylation, the electrodes were transferred to a 3.5 mL borate buffer that had been purged with nitrogen, and the radical polymerization at the surface of the acryloylated HRP was initiated by adding 30 μL aqueous solution containing 3 mg ammonium persulfate and 3 μL of *N,N,N',N'*-tetramethylethylenediamine for 1 h. To the resultant solution, acrylamide monomers and *N,N'*-methylene bisacrylamide (molar ratio = 10:1), dissolved in 0.5 mL water, were incrementally added within 1 h. The polymerization reaction was allowed to undergo for another 1 h under nitrogen. The as-prepared electrodes were stored in PBS (pH = 7.4) at 4 °C.

The wired HRP/polymer electrode was prepared following the user manual (BAS).³⁵ Briefly, 0.5 μL of a surfactant solution was cast onto the electrode surface with a microsyringe. Upon drying, the electrode was coated with 0.5 μL of the HRP/polymer solution and allowed to dry overnight. The electrode was stored in a refrigerator at 4 °C when not used.

Detection of H₂O₂ at different electrodes—For amperometric detection of H₂O₂ at the wired HRP/polymer electrode, 0.1 V vs. Ag/AgCl was applied while the sample, injected via a six-port rotary valve (Valco, Houston, TX) into a 50 mM KClO₄ solution, was delivered by a syringe pump (Kd Scientific, Holliston, MA) at 0.1 mL/min. At 0.1 V, the mediator, osmium bis(2,2'-bipyridine) chloride (Os(bpy)₂Cl³⁺), attached to the polystyrene polymer, is reduced via an electrocatalytic cycle that converts H₂O₂ to H₂O.¹¹ For H₂O₂ detection at electrodes modified with FcC₁₁SH/encapsulated HRP and its counterpart without HRP encapsulation, the experiments were conducted by holding the electrode potential at 0.5 V.

To evaluate the stability of the electrodes modified with FcC₁₁SH/encapsulated HRP, after amperometric measurements of at least five injections of 1.0 nM H₂O₂, the electrodes were stored in PBS (pH 7.4) at 4 °C before the tests in the following days.

Real sample preparation and analysis—The neuroblastoma B104 cells, kindly donated by Dr. V. Pikov at Huntington Medical Research Institute (Pasadena, CA), can also be obtained from American Type Culture Collection (Manassas, VA). Cells were seeded onto plates or dishes in Dulbecco's modified Eagle's medium (DMEM, Mediatech, Manassas, VA) supplemented with 100 U penicillin and 100 $\mu\text{g/mL}$ streptomycin at 37 °C in a humidified atmosphere of 5 % CO_2 and 95 % air. Cells were plated at the density of 5×10^3 cells and adhered onto the 96-well plates. H_2O_2 (0.5 μM) was added to the plates and after 24 h of incubation an aliquot of the cell culture was injected into the flow cell for determining the remaining H_2O_2 . H_2O_2 in a cell-free medium was also measured to assess the matrix effect on the electrochemical H_2O_2 detection. Concurrent with the cell incubation in the presence of H_2O_2 , cell viability (cytotoxicity) was evaluated through the standard MTT (3-(4,5-dimethylthiazol-2-yl)-2,5-diphenyltetrazolium bromide, Mediatech, Manassas, VA) assay.³⁶ Briefly, 100 μL DMEM were used to wash the residual H_2O_2 . Then 180 μL media and 20 μL of MTT (dissolved in PBS at a concentration of 5 mg/mL) were added to each well and incubated for 4 h at 37 °C in dark. When taken up by living cells, MTT is converted to a water-insoluble blue product (formazan). The formazan product was dissolved by adding 150 μL DMSO to each well. The absorption value at 595 nm was determined with a Tecan Genios plate reader (Tecan USA, Durham, NC). All measurements were performed in triplicates, and the cell viability was presented as the percentage of survival relative to that in control culture.

Results and Discussion

Scheme 1 depicts the general steps for modifying Au electrodes with mixed monolayers of FcC_{11}SH and encapsulated HRP. First, a mixed monolayer of FcC_{11}SH and mercaptopropionic acid (MPA) with a desired FcC_{11}SH surface coverage is self-assembled onto a gold electrode (step a). Subsequently, HRP molecules are attached to the MPA moieties via amine coupling with the NHS/EDC chemistry (steps b and c). Encapsulation of the HRP molecules is accomplished by first acryloylating the amine groups remaining on the HRP molecule, followed by radical polymerization of the acrylamide monomers (step d) around HRP.

Key to the successful construction of the monolayer of FcC_{11}SH /encapsulated HRP for electrochemical detection of H_2O_2 is that the chain length of the ferrocenylalkanethiol must be longer than that of the carboxyl-terminated alkanethiol. This allows the Fc groups to be in close proximity of HRP. In addition, the ratio of FcC_{11}SH /HRP (or that of FcC_{11}SH /MPA in the first step) should be optimized. Consequently HRP molecules are surrounded by FcC_{11}SH and the electron transfer between HRP and H_2O_2 can be effectively mediated by FcC_{11}SH . We found that mixed monolayers containing 7–15% of FcC_{11}SH (estimated from charges under the ferrocene oxidation peaks) produce high electrocatalytic currents. FcC_{11}SH surface coverage in this range can be regulated either by controlling the molar ratio between FcC_{11}SH and MPA solutions used for the mixed monolayer formation or using MPA to partially replace a preformed mixed monolayer of FcC_{11}SH /MPA (*cf.* details in Experimental Section). Rubín et al. found that 7% of 16-ferrocenylhexadecanethiol in a mixed monolayer that also contains glucose oxidase yields the highest sensitivity towards glucose detection.³⁷ The coverage of FcC_{11}SH in the mixed monolayer is relatively low for the optimal signal, because the enzyme molecules are much bulkier than FcC_{11}SH and only the Fc groups positioned next to the enzyme molecules are capable of mediating the electron transfer. We should mention that Liu and coworkers have shown that HRP encapsulated in a homogeneous solution has a typical shell thickness between 2 and 5 nm.²⁶ Such a thickness is sufficiently small and the electron transfer between FcC_{11}SH and HRP is therefore not impeded. The electron transfer between the electrode and the Fc moieties is known to be facile when the alkanethiol linker is not particularly long.^{38, 39} The mediated electron transfer is analogous to that occurs to a monolayer of redox active proteins immobilized onto an alkanethiol layer (*i.e.*, monolayer protein voltammetry^{40, 41}).

Traditionally, mediated electrochemical detection of H_2O_2 utilizing an HRP-modified electrode and a mediator (M) in solution, can be generalized using notations similar to those in a recent review by Heller and Feldman:⁴²



where HRP^+ represents the oxidized form of HRP and M^+ denotes the oxidized form of the mediator. When M is Fc or a Fc derivative in solution, by setting the electrode potential at a value (typically < 0.3 V vs. $\text{Ag}/\text{AgCl}^{33}$) to reduce the enzymatically generated Fc^+ back to Fc, the catalytic cycle continuously converts H_2O_2 to H_2O . The commercially successful wired HRP/polymer electrode utilizing $\text{Os}(\text{bpy})_3^{2+}$ as the mediator follows the same electrode reaction.¹¹ However, we did not observe any electrocatalytic current when the as-prepared electrode was held at such a potential. Rather, considerably high oxidation current was observed when a potential greater than 0.5 V was applied. At 0.5 V or beyond, the Fc group at the end of the alkyl chain is oxidized (*cf.* solid line curve in Figure 1). The oxidation potential of FcC_{11}SH , taken as the average of the anodic (0.43 V) and cathodic (0.39 V) peak potentials, is 0.41 V. When HRP was added into a PBS solution housing an $\text{FcC}_{11}\text{SH}/\text{MPA}$ -modified electrode, we observed an increase in the anodic peak (*cf.* dashed line curve in Figure 1). Addition of H_2O_2 further increased the anodic peak and reduced the cathodic peak (dotted line curve). These behaviors are also characteristic of an electrocatalytic reaction (EC' mechanism⁴³).

A number of papers have shown that, in the presence of an oxidant, HRP can be first oxidized to a form that contains a four-valent Fe center (i.e., oxypoxidase^{44–46}) and is capable of oxidizing H_2O_2 to O_2 . This form, denoted herein as $\text{Fe}(\text{IV})\text{-HRP}$ or HRP^{2+} , may be responsible for the observed electrocatalytic oxidation of H_2O_2 :



where Red is the reduced form of the oxidant that is capable of oxidizing HRP to the $\text{Fe}(\text{IV})\text{-HRP}$. From the dashed line curve in Figure 1, it is evident that the oxidized FcC_{11}SH at the electrode, viz., $\text{Fc}^+\text{C}_{11}\text{SH}$, can oxidize HRP. Therefore, we suggest that $\text{Fc}^+\text{C}_{11}\text{SH}$ may behave as an oxidant and has converted the surface-confined HRP to its oxidized form HRP^{2+} . The regeneration of FcC_{11}SH explains the increase of anodic current from the solid to the dashed line curves. In the presence of H_2O_2 , HRP^{2+} oxidizes H_2O_2 to O_2 and itself is converted back to the native HRP. Thus, the anodic current is further amplified (*cf.* the dotted line curve in Figure 1).

The above mechanism is reasonable considering that the potential of oxypoxidase or HRP²⁺ is approximately between 0.5 and 0.7 V,⁴⁷ which is quite close to the oxidation potential of Fc⁺C₁₁SH. This is also close to the diffusion-limited oxidation of H₂O₂ to O₂ at Pt electrodes.^{11, 48} The close proximity between FcC₁₁SH and HRP molecules at the electrode may have lowered the energy barrier for the electron transfer. Thus, achieving H₂O₂ oxidation at a less positive potential at an electrode less catalytic than Pt is an attractive aspect of the as-prepared electrode. To provide further support to the above mechanism, we conducted another experiment by employing Ru(bpy)₃²⁺ whose oxidation potential is rather high (1.11 V vs. Ag/AgCl⁴³). When HRP is present in the solution, a sigmoidal CV of Ru(bpy)₃²⁺ was observed (See the dashed voltammogram in Figure 2). In the presence of H₂O₂, the increase in the steady-state anodic current is even more pronounced (dotted line curve). In this case, the electrogenerated Ru(bpy)₃³⁺ acts as an oxidant in the same fashion as Fc⁺C₁₁SH to facilitate the HRP-catalyzed electrooxidation of H₂O₂ to O₂. Overall, the lack of a H₂O₂ reduction reaction is not entirely surprising, given that the potentials of redox proteins in thin films depend on a variety of factors such as the substrate electrode, the interaction of the proteins with the film materials, and the identity of the redox proteins.^{49, 50}

When HRP is immobilized and encapsulated, the oxidation current corresponding to the co-immobilized FcC₁₁SH increases with H₂O₂ (Figure 3). Such a behavior is in remarkable resemblance to that obtained with HRP in solution (*cf.* Figure 1 and Figure 2). Thus, we conclude that the FcC₁₁SH/encapsulated HRP electrode can efficiently catalyze the oxidation of H₂O₂ and encapsulating HRP does not appear to hinder (1) the diffusion of H₂O₂ from the solution to the HRP molecules and (2) the facile electron transfer reaction between Fc⁺C₁₁SH and HRP. We should note that H₂O₂ detection is often accomplished by using electrodes modified with various oxidases.^{50, 51} These electrodes generally require O₂ for sustained enzymatic function. Thus, the generation of O₂ from the electrocatalytic oxidation of H₂O₂ could potentially help prevent oxygen depletion in various detection schemes.

The amperometric detection of H₂O₂ in a thin-layer flow cell housing an FcC₁₁SH/encapsulated HRP electrode was optimized. We found that, in the range of flow rates studied (0.015–0.14 mL/min), 0.080 mL/min produced the highest current (data not shown). This is understandable, as a higher flow rate increases the mass transfer rate of H₂O₂. But as the flow rate becomes too high, the reaction time becomes rather short and the effect outweighs the contribution by the increased mass transfer at a high flow rate. We also studied the dependence of the electrocatalytic current on solution pH (filled squares in Figure 4) and compared the behavior observed at a wired HRP/polymer electrode (open circles). Two points are worth noting: (1) both types of HRP electrodes possess enzymatic activity across a wide pH range (5.0–10.0 for the FcC₁₁SH/encapsulated HRP electrode and 4.0–8.0 for the wired HRP/polymer electrode), and (2) the pH dependence of the wired HRP/polymer electrode is opposite to that of the FcC₁₁SH/encapsulated HRP electrode. The pH dependences of these two types of electrodes can be rationalized by the difference between the aforementioned mechanisms. For the HRP-catalyzed H₂O₂ reduction (*cf.* eq. 1), the equation

$E_{H_2O_2/H_2O} = E_{H_2O_2/H_2O}^0 + 0.0296 \log [H_2O_2] - 0.0592 \text{pH}$ describes the pH dependence of redox potential of the H₂O₂/H₂O couple. As such, an increase in pH would decrease the potential or the oxidizing power of H₂O₂. The net effect is a decrease in the mediator (Os(bpy)₃²⁺) turn-over rate or catalytic current. On the contrary, for HRP-catalyzed H₂O₂ oxidation (*cf.* eq. 7), H₂O₂ is oxidized and the potential of the redox couple O₂/H₂O₂ is also pH dependent ($E_{O_2/H_2O_2} = E_{O_2/H_2O_2}^0 - 0.0296 \log [H_2O_2] - 0.0592 \text{pH}$). In this case, an increase in pH would also decrease the potential, but the reducing power of H₂O₂ is increased. As the consequence, the driving force of redox reaction 7 is increased and the Fc⁺C₁₁SH mediator turn-over rate is higher. Notice that the current begins to level off at pH < 5.0 and > 9.0 at the wired HRP/polymer and the FcC₁₁SH/encapsulated HRP electrodes, respectively. In both cases, the

electrocatalytic currents are governed by the mass transfer of H_2O_2 from the bulk solution to the electrode surface. The contrast in the pH dependences again strongly suggests that H_2O_2 is oxidized at the electrode prepared in this work.

Having optimized the experimental condition, we performed amperometric detection of H_2O_2 across a wide range of concentrations. Figure 5A depicts a representative chronoamperogram showing three consecutive injections of three different H_2O_2 concentrations. It is clear that reproducible peaks can be obtained and the peak height is proportional to the three concentrations. From the variations of the baseline signals, we estimated the detection limit (3σ) for H_2O_2 at this electrode to be 0.64 nM. This is a reasonable detection limit since injections of 1.0 nM H_2O_2 produced well-resolved peaks with a good signal-to-noise ratio (*cf.* inset of Figure 5A). Figure 5B displays the calibration plot for $[\text{H}_2\text{O}_2]$ between 1.0 nM and 100 μM and the inset shows the linear portion of the plot (from 1.0 nM to 1.6 μM). The dynamic range is comparable to that obtained at the wired HRP/polymer electrode (from 0.50 nM to 1.0 μM). The excellent linearity ($R^2 = 0.999$) suggests that the dynamic range spans over three orders of magnitude and the RSD values range within 1.3–4.1%, which are considered to be excellent.⁵² We also assessed the reproducibility among three different electrodes. The RSD value (3.4%) is also rather small and the difference can be attributed to the slight variation in the FcC_{11}SH coverage among different electrodes. At the wired HRP/polymer electrode, the detection limit was found to be lower (0.033 nM). The lower detection limit is expected, because the 3-D polymer network can incorporate more mediator and enzyme molecules⁵¹ than the mediator and enzyme molecules dispersed in a 2-D mixed monolayer. However, we should point out that the calibration curve for the wired HRP/polymer electrode deviates from linearity at H_2O_2 concentration below 0.5 nM. Thus the detection limit is not much lower than that of the FcC_{11}SH /encapsulated HRP electrode.

Figure 6 is a bar graph comparing the durability among the three types of electrodes, viz., the FcC_{11}SH /encapsulated HRP electrode (red), the FcC_{11}SH /HRP electrode (green), and the wired HRP/polymer electrode (blue). It is apparent that both the wired HRP/polymer and the FcC_{11}SH /HRP (i.e., HRP is not encapsulated) begin to degrade after about three days. The stability of the wired HRP/polymer electrode is consistent with the one-week shelf life noted by the vendor.³⁵ In contrast, the FcC_{11}SH /encapsulated HRP electrode remains stable for almost three weeks and only loses 16% of its catalytic efficiency after 21 days.

To determine whether the retention of catalytic activity of HRP is due to the preservation of the native structure or due to the isolation of the HRP from the sample solution by the hydrogel, we also modified electrodes with native and denatured HRP molecules and subsequently covered them with a poly-L-lysine (PLL) film. Specifically, following the attachment of HRP onto the MPA/ FcC_{11}SH mixed monolayer (*cf.* Scheme 1) PLL was cross-linked using the NHS/EDC chemistry. In a separate experiment, an electrode covered with FcC_{11}SH /HRP was immersed in a 15% methanol solution at 60 °C for 20 min to denature HRP, which was followed by attachment of the PLL matrix. While the former electrode showed excellent amperometric response to injected H_2O_2 , essentially no signals were detected at the latter electrode. In addition, we found that denatured HRP that had been encapsulated also did not produce electrocatalytic currents. Since Rusling and coworkers have demonstrated that enzymes such as HRP can retain near native structures for extended periods when cross-linked to PLL films,¹⁴ the above observations suggest that encapsulation of HRP renders an environment that retains the native structure of HRP and prolongs its enzymatic activity.

Finally, we applied the FcC_{11}SH /encapsulated HRP electrode to the detection of H_2O_2 in a real sample. In neuroscience research, reactive oxygen species such as H_2O_2 are widely believed to cause oxidative stress/damage to cells.⁵³ H_2O_2 or species that produce H_2O_2 are generally introduced to neuronal cell cultures and cell viability is monitored over a period of

time.^{36, 54, 55} For example, we^{56, 57} and others^{58, 59} have shown that redox metals (e.g., Cu^{2+} and Fe^{3+}), upon complexation with amyloid peptides, can generate H_2O_2 with cellular redox species. Knowledge about the percent of H_2O_2 along the course of incubation affords accurate information about the dosage of H_2O_2 that inflicts cell death. To demonstrate the viability of using the FcC_{11}SH /encapsulated HRP electrode for H_2O_2 detection in a complex sample matrix, we first spiked a cell-free medium with 500.0 nM H_2O_2 and determined the amount of H_2O_2 to be 494.4 ± 5.7 nM (RSD = 1.14%). The excellent accuracy also demonstrates that the cell culture matrix does not cause appreciable surface contamination and degradation of the HRP activity and the various species in the culture medium do not react with H_2O_2 . In a separate experiment, we added 500.0 nM H_2O_2 into a B104 neuroblastoma cell culture sample, and, through a MTT assay³⁶ (see also details in Experimental Section), found that only 45% of the cells survived after 20 h. The injection peaks presented by the dashed line curve in Figure 7 clearly show that H_2O_2 remaining in the cell culture can be detected rapidly and reproducibly (RSD = 0.82% for the three injection peaks). The H_2O_2 concentration was determined to be 188.1 ± 1.1 nM, which is in excellent agreement with that obtained at the wired HRP/polymer electrode (197.8 ± 3.3 nM). The remaining H_2O_2 is about 38% of the original dosage, suggesting that a large fraction of the original dosage has reacted and caused the cell death. From this experiment, we conclude that encapsulation of the HRP molecule affords reliable analyses for H_2O_2 in biological samples.

Conclusion

Gold electrodes modified with mixed monolayers of FcC_{11}SH /encapsulated HRP have been successfully applied to the amplified amperometric detection of H_2O_2 at trace levels. By electrogenerating ferrocenium at the end of an alkanethiol tether, a catalytic cycle is created, which results in an increased oxidation current or signal amplification. The electrode process was elucidated to be an HRP-catalyzed oxidation reaction of H_2O_2 to O_2 . Construction of the FcC_{11}SH /encapsulated HRP electrode is straightforward and the electrode performance was optimized by studying the influences of FcC_{11}SH surface coverage, solution pH, and flow rate on the amplified signals. The dynamic range and sensitivity are highly comparable to those achievable with the commercially available wired HRP/polymer electrode. The as-prepared electrode yields a detection limit of 0.64 nM, which is quite remarkable considering that both the enzyme and mediator molecules are spread in a monolayer (instead of across a thick film). Compared to electrodes at which HRP molecules are exposed, the encapsulation of the preimmobilized HRP is demonstrated to enhance the durability of the electrode and to render the amenability to detection of H_2O_2 in complex sample matrix. The significantly improved stability can be ascribed to the porous acrylonated exterior formed at the surface of HRP molecules, which allows H_2O_2 to reach the HRP core while retaining the native structure of the HRP molecule.

Acknowledgments

Partial support of this work by an NIH-NINDS grant (No: 1SC1NS070155-01 to FZ), the RIMI Program at California State University, Los Angeles (P20-MD001824-01 to FZ), a NSF-RUI grant (No. 0555224 to FZ), and the Natural Science Foundation of China (Nos. 20676153 and 20876179 to YL) is gratefully acknowledged. YP also thanks the China Scholarship Council for financial support.

Reference

1. Zhang, X.; Ju, H.; Wang, J., editors. *Electrochemical Sensors, Biosensors and their Biomedical Applications*. New York: Academic Press; 2007.
2. Cooper, J.; Cass, T., editors. *Biosensors*. Vol. 2nd ed.. Oxford: Oxford University Press; 2004.
3. Ramsay, G., editor. *Commercial Biosensors: Applications to Clinical, Bioprocess, and Environmental Samples*. New York: Wiley-Interscience; 1998.

4. Borisov SM, Wolfbeis OS. *Chem. Rev* 2008;108:423–461. [PubMed: 18229952]
5. Wang J. *Chem. Rev* 2008;108:814–825. [PubMed: 18154363]
6. Privett BJ, Shin JH, Schoenfisch MH. *Anal. Chem* 2008;80:4499–4517. [PubMed: 18491869]
7. Wang G, Xu JJ, Chen HY, Lu ZH. *Biosens. Bioelectron* 2003;18:335–343. [PubMed: 12604250]
8. Kang X, Wang J, Tang Z, Wu H, Lin Y. *Talanta* 2009;78:120–125. [PubMed: 19174213]
9. Holtz JH, Asher SA. *Nature* 1997;389:829–832. [PubMed: 9349814]
10. Yu X, Sotzing GA, Papadimitrakopoulos F, Rusling JF. *Anal. Chem* 2003;75:4565–4571. [PubMed: 14632065]
11. Yang L, Janle E, Huang TH, Gitzen J, Kissinger PT, Vreeke M, Heller A. *Anal. Chem* 1995;67:1326–1331.
12. Ma D, Li M, Patil AJ, Mann S. *Adv. Mater* 2004;16:1838–1841.
13. Kumar R, Maitra AN, Patanjali PK, Sharma P. *Biomaterials* 2005;26:6743–6753. [PubMed: 15951014]
14. Guto PM, Kumar CV, Rusling JF. *J. Phys. Chem. B* 2007;111:9125–9131. [PubMed: 17608411]
15. Russell RJ, Pishko MV, Simonian AL, Wild JR. *Anal. Chem* 1999;71:4909–4912. [PubMed: 10565282]
16. Lahiri J, Isaacs L, Tien J, Whitesides GM. *Anal. Chem* 1999;71:777–790. [PubMed: 10051846]
17. Wei X, Cruz J, Gorski W. *Anal. Chem* 2002;74:5039–5046. [PubMed: 12380828]
18. Liu Y, Wang MK, Zhao F, Xu ZA, Dong SJ. *Biosens. Bioelectron* 2005;21:984–988. [PubMed: 16257668]
19. Stevens MM, Allen S, Davies MC, Roberts CJ, Schacht E, Tendler SJB, VanSteenkiste S, Williams PM. *Langmuir* 2002;18:6659–6665.
20. Sigal GB, Bamdad C, Barberis A, Strominger J, Whitesides GM. *Anal. Chem* 1996;68:490–497. [PubMed: 8712358]
21. Schoenfisch MH, Rothrock AR, Shin JH, Polizzi MA, Brinkley MF, Dobmeier KP. *Biosens. Bioelectron* 2006;22:306–312. [PubMed: 16483759]
22. Yu BZ, Long N, Moussy Y, Moussy F. *Biosens. Bioelectron* 2006;21:2275–2282. [PubMed: 16330201]
23. Moattisirat D, Poitout V, Thome V, Gangnerau MN, Zhang Y, Hu Y, Wilson GS, Lemonnier F, Klein JC, Reach G. *Diabetologia* 1994;37:610–616. [PubMed: 7926347]
24. Heitner-Wirguin C. *J. Membr. Sci* 1996;120:1–33.
25. Kim J, Grate JW. *Nano Lett* 2003;3:1219–1222.
26. Yan M, Ge J, Liu Z, Ouyang PK. *J. Am. Chem. Soc* 2006;128:11008–11009. [PubMed: 16925402]
27. Liu GD, Lin YH, Ostatna V, Wang J. *Chem. Commun* 2005:3481–3483.
28. Kenausis G, Chen Q, Heller A. *Anal. Chem* 1997;69:1054–1060. [PubMed: 9075402]
29. Mulchandani A, Pan ST. *Anal. Biochem* 1999;267:141–147. [PubMed: 9918666]
30. Patolsky F, Zayats M, Katz E, Willner I. *Anal. Chem* 1999;71:3171–3180. [PubMed: 10450161]
31. Su XD, O'Shea SJ. *Anal. Biochem* 2001;229:241–246. [PubMed: 11730349]
32. Castillo J, Gaspar S, Sakharov I, Csoregi E. *Biosens. Bioelectron* 2003;705–714. [PubMed: 12706582]
33. Tatsuma T, Okawa Y, Watanabe T. *Anal. Chem* 1989;61:2352–2355.
34. Schmidt A, Schumacher JT, Reichelt J, Hecht HJ, Bilitewski U. *Anal. Chem* 2002;74:3037–3045. [PubMed: 12141662]
35. <http://www.basinc.com/mans/PE-man.pdf>
36. Lin YC, Huang YC, Chen SC, Liaw CC, Kuo SC, Huang LJ, Gean PW. *Neurochem. Res* 2009;34:923–930. [PubMed: 18841465]
37. Rubin S, Chow JT, Ferraris JP, Zawodzinski TA. *Langmuir* 1996;12:363–370.
38. Creager SE, Weber K. *Langmuir* 1993;9:844–850.
39. Smalley JF, Feldberg SW, Chidsey CED, Linford MR, Newton MD, Liu Y-P. *J. Phys. Chem* 1995;99:13141–13149.
40. Clark RA, Bowden EF. *Langmuir* 1997;13:559–565.

41. El Kasmi A, Wallace JM, Bowden EF, Binet SM, Linderman RJ. *J. Am. Chem. Soc* 1998;120:225–226.
42. Heller A, Feldman B. *Chem. Rev* 2008;108:2482–2505. [PubMed: 18465900]
43. Bard, AJ.; Faulkner, LR., editors. *Electrochemical Methods: Fundamentals and Applications*. New York: John Wiley & Sons; 2001.
44. Jenzer H, Jones W, Kohler H. *J. Biol. Chem* 1986;261:5550–5556.
45. Zhou YL, Hu NF, Zeng YH, Rusling JF. *Langmuir* 2002;18:211–219.
46. Huang R, Hu NF. *Biophys. Chem* 2003;104:199–208. [PubMed: 12834838]
47. Everse, J.; Grisham, MB.; Everse, KE., editors. *Peroxidases in Chemistry and Biology*. Boca Raton, FL: CRC Press; 1990.
48. Hu Y, Zhang Y, Wilson G. *Anal. Chim. Acta* 1993;281:503–511.
49. Rusling JF. *Acc. Chem. Res* 1998;31:363–369.
50. Rusling, JF.; Zhang, Z. *Biomolecular Films*. Rusling, JF., editor. New York: Marcel Dekker; 2003. p. 1-64.
51. Heller A. *Acc. Chem. Res* 1990;23:128–134.
52. Skoog, DA.; Holler, FJ.; Crouch, SR., editors. *Principles of Instrumental Analysis*. Vol. 6th ed.. Belmont, CA: Thomson Brooks/Cole; 2007.
53. Gaggelli E, Kozlowski H, Valensin D, Valensin G. *Chem. Rev* 2006;106:1995–2044. [PubMed: 16771441]
54. Heo SR, Han AM, Kwon YK, Joung I. *Neurosci. Lett* 2009;450:45–50. [PubMed: 19010391]
55. Baruch-Suchodolsky R, Fischer B. *Biochemistry* 2009;48:4354–4370. [PubMed: 19320465]
56. Jiang DL, Men LJ, Wang JX, Zhang Y, Chickenyen S, Wang YS, Zhou FM. *Biochemistry* 2007;46:9270–9282. [PubMed: 17636872]
57. Jiang D, Li X, Williams R, Patel S, Men L, Wang Y, Zhou F. *Biochemistry* 2009;48:7939–7947. [PubMed: 19601593]
58. Huang XD, Cuajungco MP, Atwood CS, Hartshorn MA, Tyndall JDA, Hanson GR, Stokes KC, Leopold M, Multhaup G, Goldstein LE, Scarpa RC, Saunders AJ, Lim J, Moir RD, Glabe C, Bowden EF, Masters CL, Fairlie DP, Tanzi RE, Bush AI. *J. Biol. Chem* 1999;274:37111–37116. [PubMed: 10601271]
59. Streltsov VA, Varghese JN. *Chem. Commun* 2008:3169–3171.

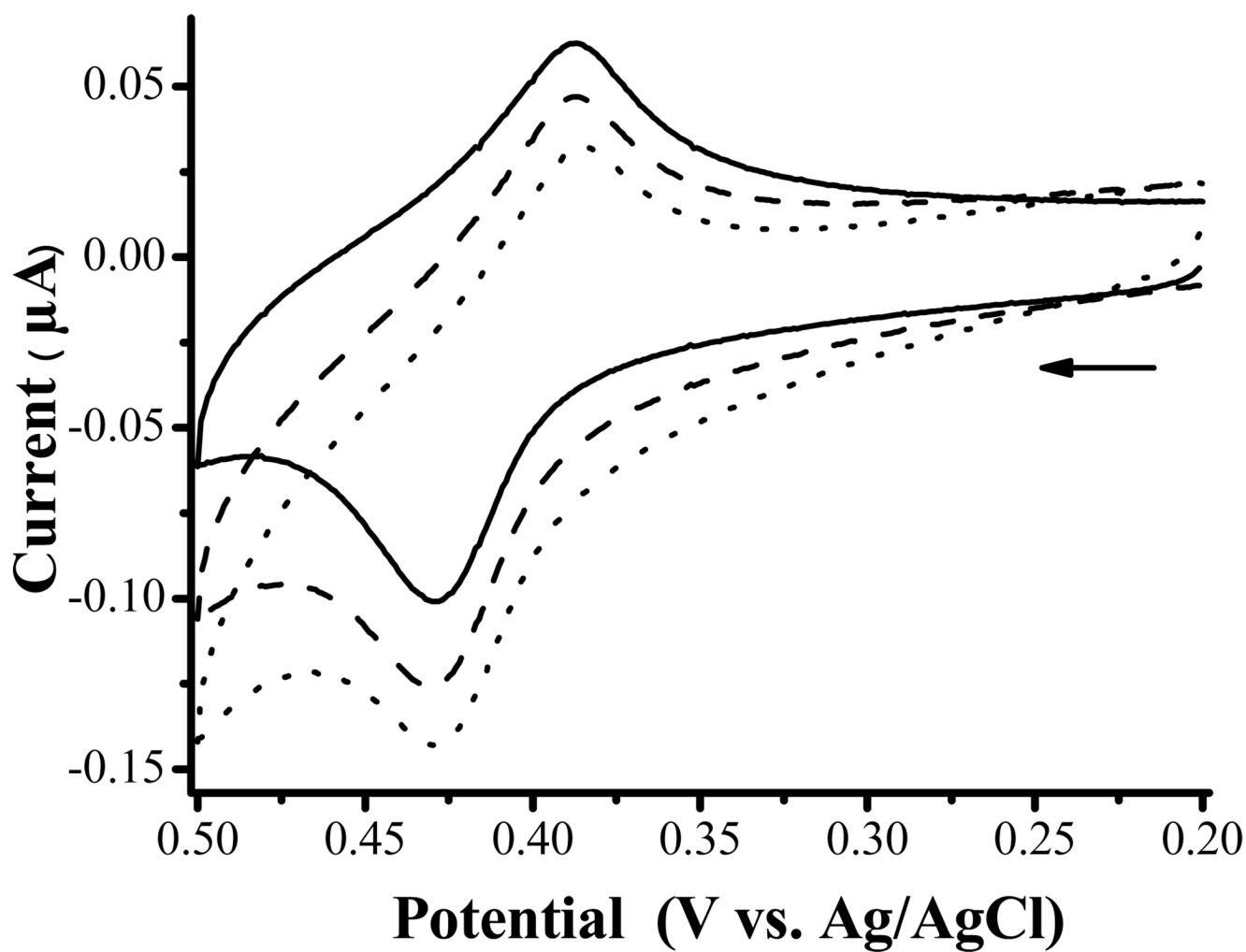


Figure 1. CVs acquired at an Au electrode modified with a mixed monolayer of FcC₁₁SH and MPA in a 0.1 M PBS solution (solid line curve), in a PBS solution containing 0.2 mM HRP (dashed) and in a PBS solution containing 0.2 mM HRP and 0.2 mM H₂O₂ (dotted). The scan rate was 5 mV/s and the arrow indicates the initial scan direction.

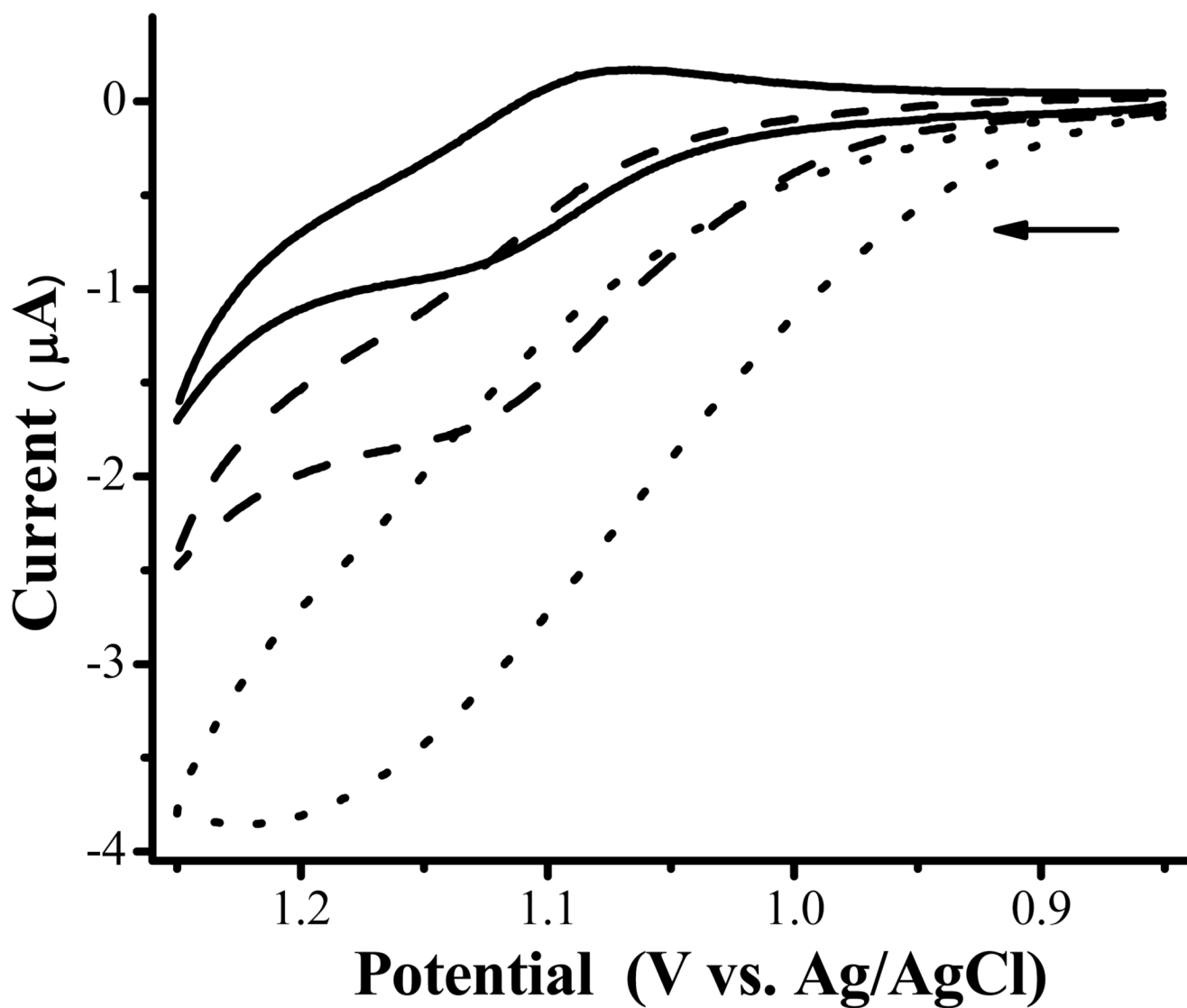


Figure 2. CVs acquired at a bare Au electrode in a PBS solution containing 0.2 mM $\text{Ru}(\text{bpy})_3^{2+}$ (solid line curve), 0.2 mM $\text{Ru}(\text{bpy})_3^{2+}$ and 0.2 mM HRP (dashed), and 0.2 mM $\text{Ru}(\text{bpy})_3^{2+}$, 0.2 mM HRP, and 0.2 mM H_2O_2 (dotted). The scan rate was 5 mV/s and the arrow indicates the initial scan direction.

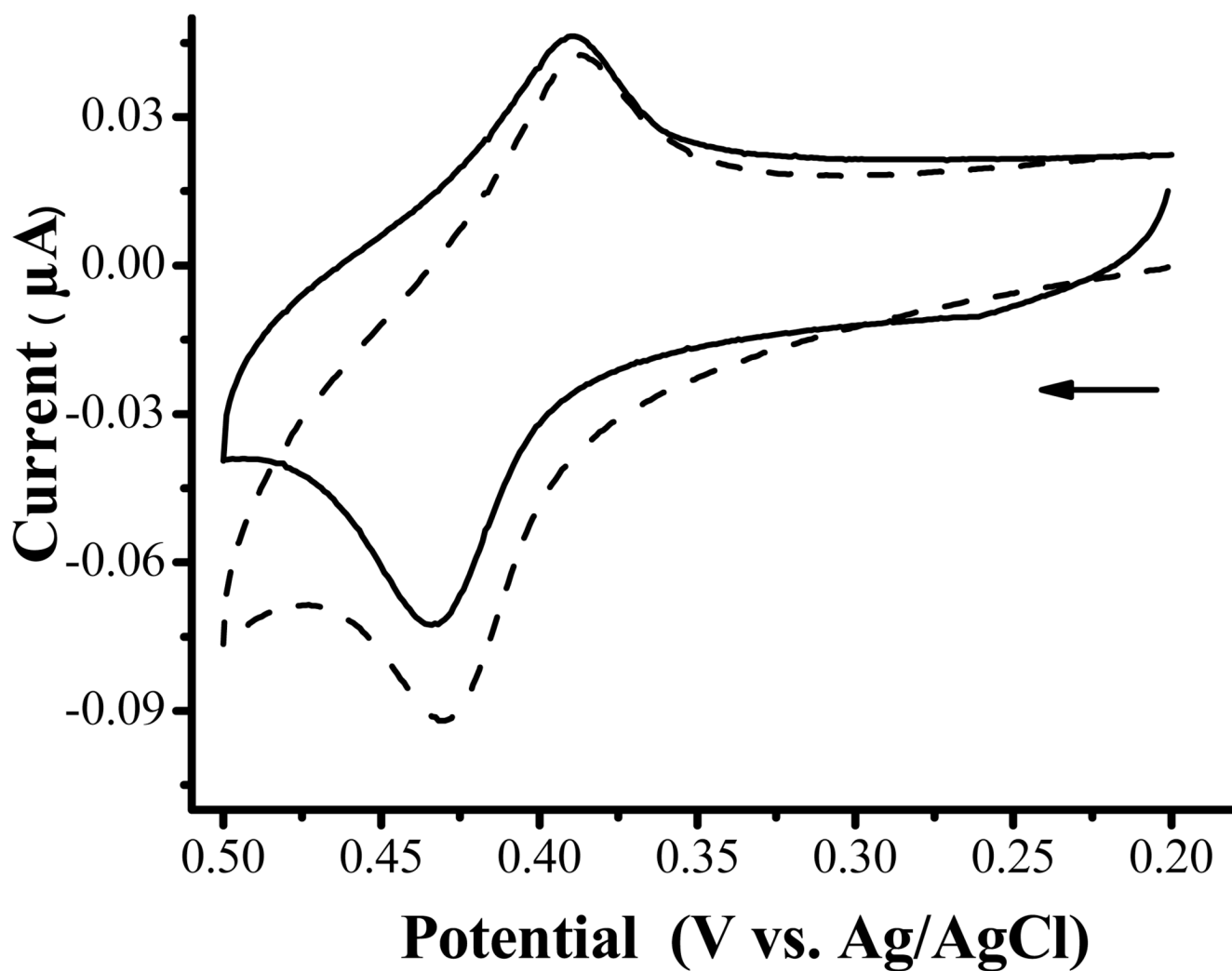


Figure 3. CVs at a mixed monolayer of FcC₁₁SH/encapsulated HRP acquired in 0.1 M PBS (solid line curve) and PBS containing 20 μM H₂O₂ (dashed). Scan rate = 5 mV/s and the arrow indicates the initial scan direction.

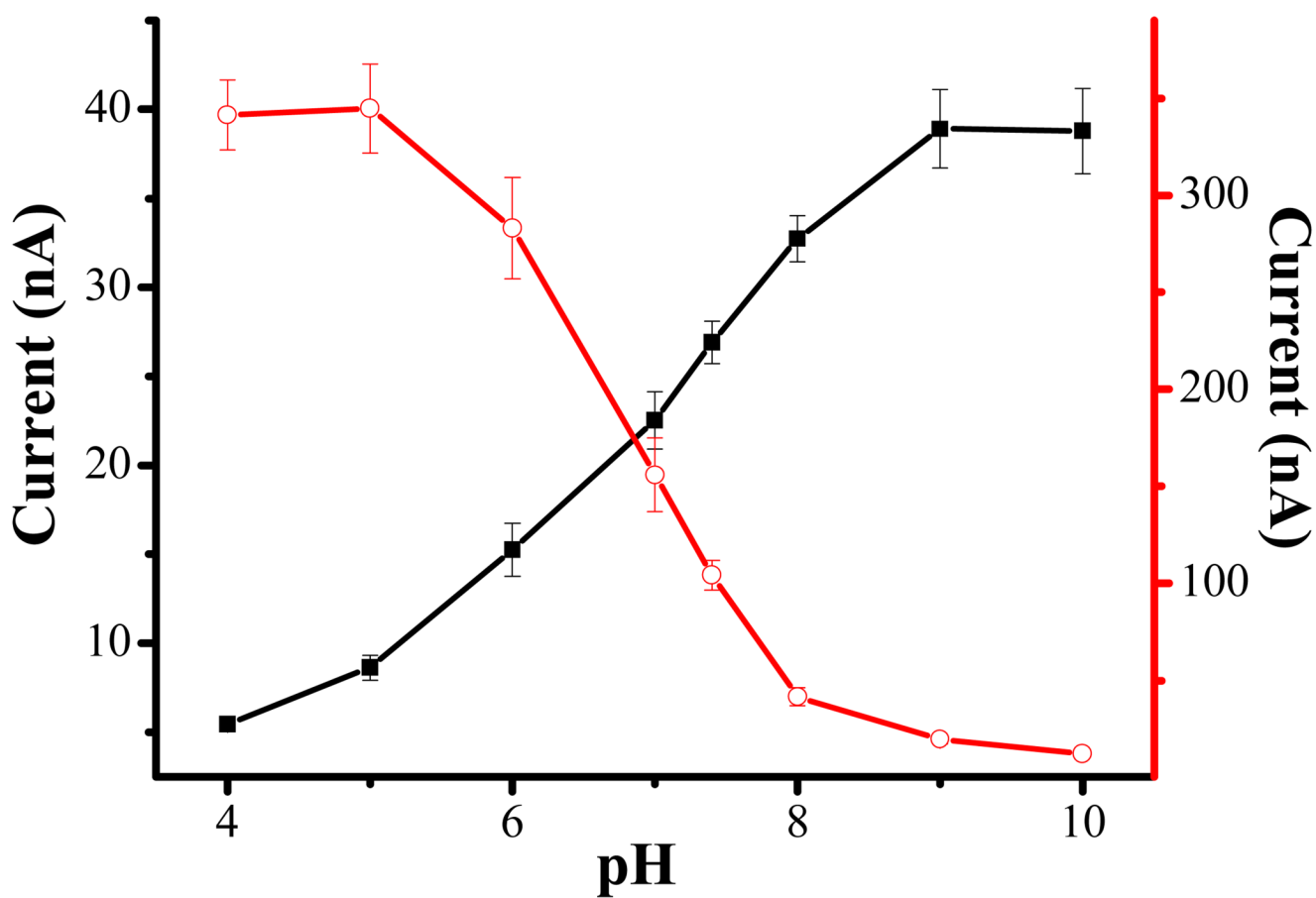


Figure 4. Dependence of electrocatalytic currents on solution pH: currents recorded at a wired HRP/polymer electrode (open circles) and the FcC₁₁SH/encapsulated HRP electrode (filled squares). For both electrodes, 1 μ M H₂O₂ was used. RSD values ranging from 1.86 to 10.2% are plotted as the error bars (n = 3).

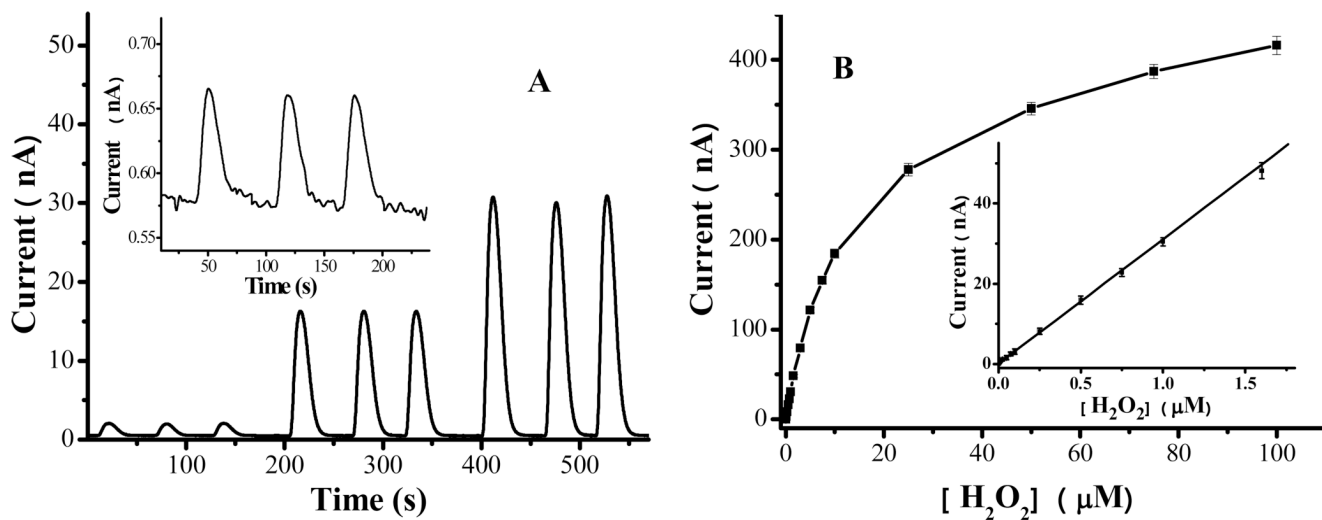


Figure 5.

(A) Amperometric response at an FcC_{11}SH /encapsulated HRP electrode upon consecutive injections of three different H_2O_2 concentrations (0.05, 0.50 and 1.0 μM). The electrode was held at 0.5 V vs. Ag/AgCl, while the injected H_2O_2 samples were delivered at 0.08 mL/min. Inset: Amperometric response to three consecutive injections of 1.0 nM H_2O_2 . (B) Dependence of the electrocatalytic current on $[\text{H}_2\text{O}_2]$ in the range between 1 nM and 100 μM , i (nA) = 0.029 $[\text{H}_2\text{O}_2]$ (nM) + 0.56 (nA). The inset shows the linear portion of the plot ($r^2 = 0.999$ between 1.0 nM and 1.6 μM). Each concentration was repeated three times and the error bars represent the RSD values.

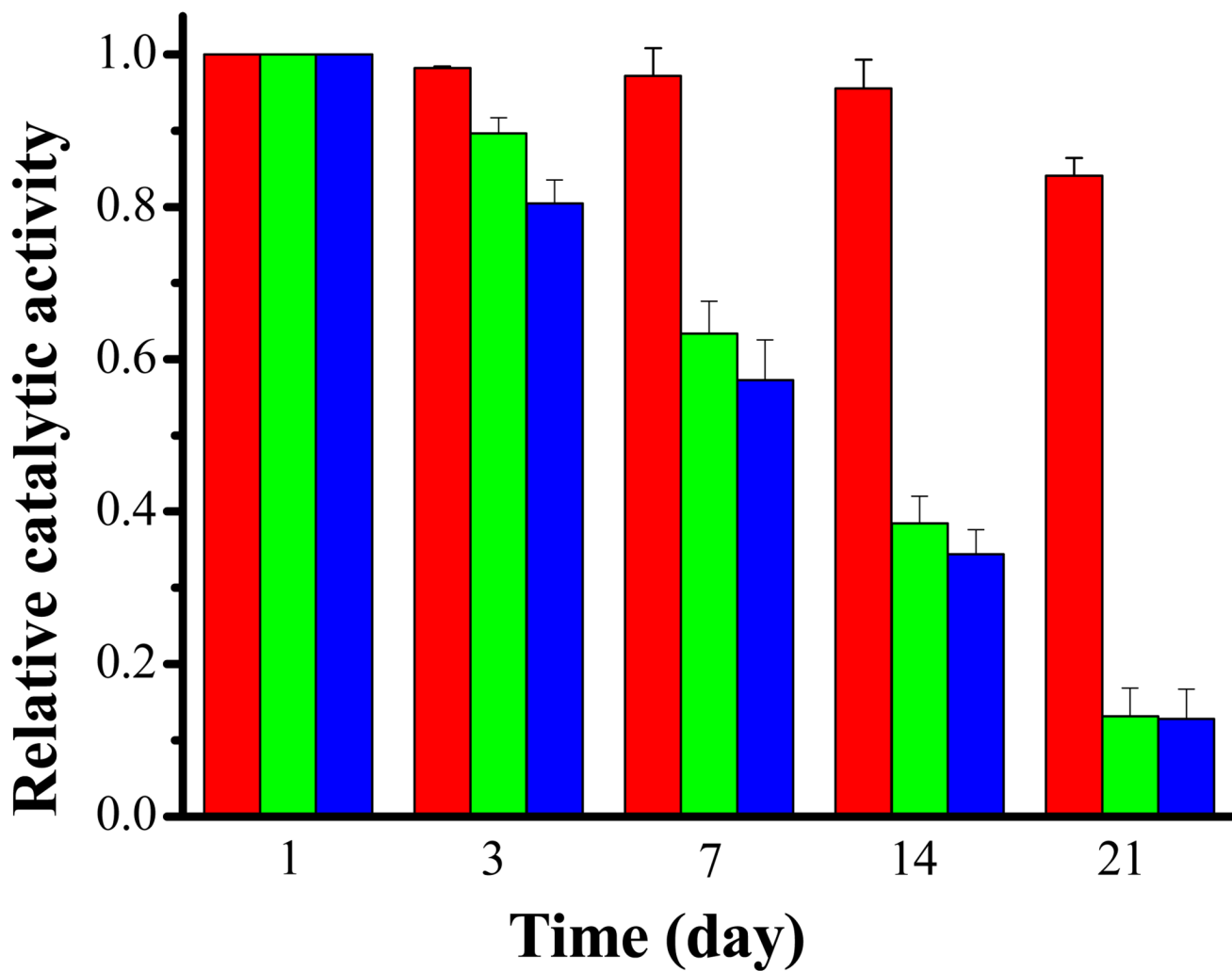


Figure 6. Comparison of stability among the FcC₁₁SH/encapsulated HRP electrode (red), the FcC₁₁SH/HRP electrode (green), and the wired HRP/polymer electrode (blue). Error bars represent the RSD values (n = 3), which range between 0.14 and 8.1%.

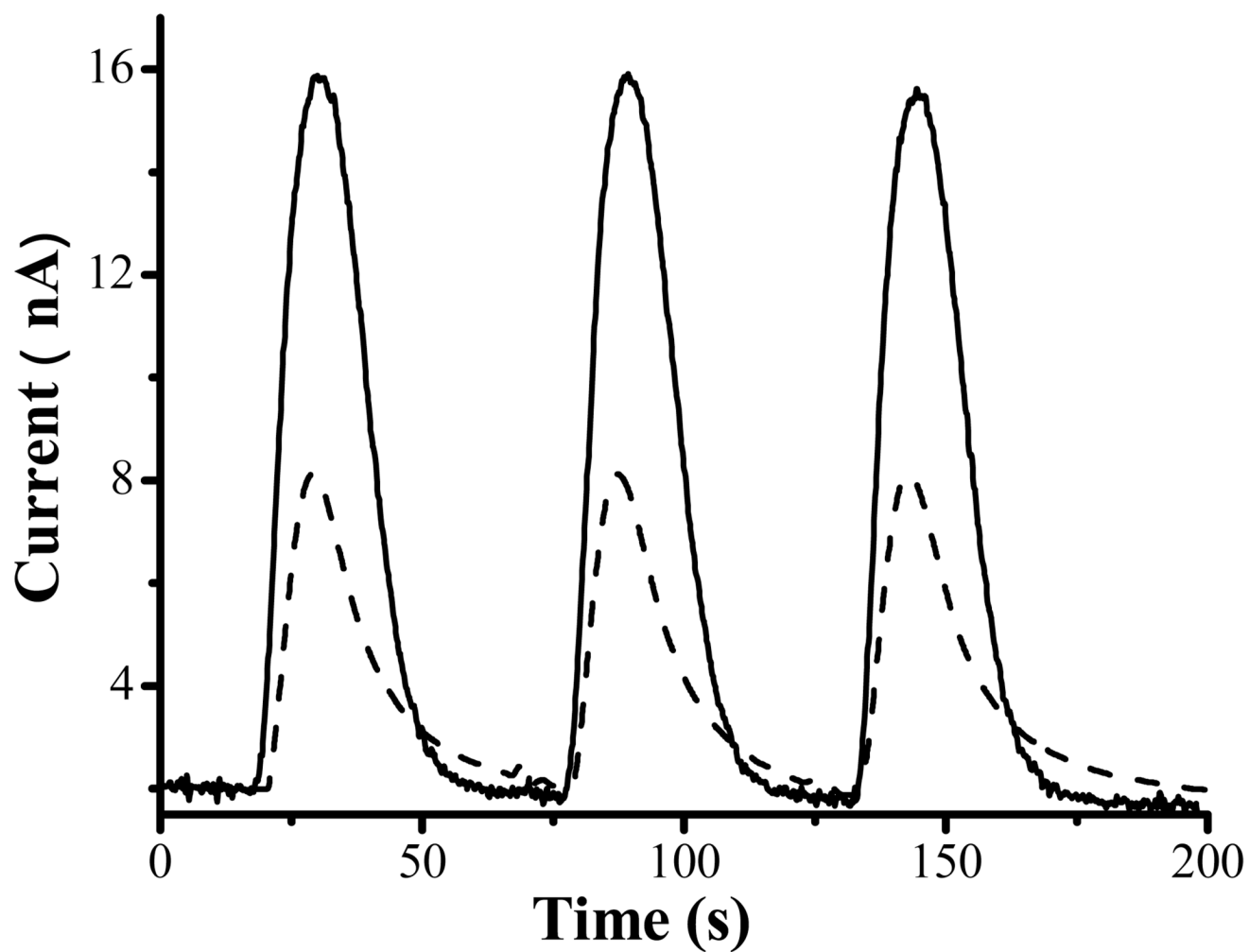
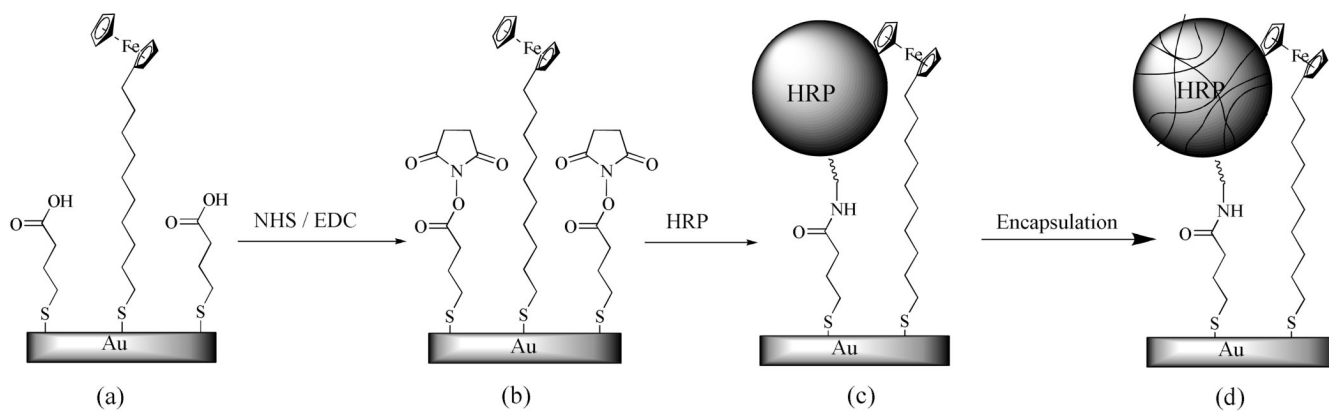


Figure 7.

Amperometric responses corresponding to three consecutive injections of a cell-free medium containing 500 nM H_2O_2 (solid line curve) and the medium containing B-104 neuroblastoma that had been incubated with 500 nM H_2O_2 for 20 h (dashed). The flow rate used was 0.08 mL/min and the electrode potential was held at 0.5 V vs. Ag/AgCl.

**Scheme 1.**

Steps for constructing the mixed monolayer of FcC₁₁SH and encapsulated HRP at a Au electrode: (a) formation of a mixed monolayer of MPA/FcC₁₁SH, (b) activation of and NHS ester attachment onto MPA, (c) cross-linking of HRP, and (d) encapsulation of HRP through acryloylation. For illustration, the molecules are not drawn to scale.